Bulgarian Chemical Communications, Volume 49, Special Issue F, (pp. 51 - 58) 2017

Silver and quercetin loaded nanostructured silica materials as potential dermal formulations

I. Trendafilova[1]*, D. Momekova[2], A. Szegedi[3], G. Momekov[2], D. Zgureva[4], S. Boycheva[4], M. Popova[1]

[1]*Institute of Organic Chemistry with Centre of Phytochemistry, Bulgarian Academy of Sciences, 1113 Sofia, Bulgaria*
[2] *Faculty of Pharmacy, Medical University of Sofia, 2 Dunav Str., 1000 Sofia, Bulgaria*
[3] *Research Centre for Natural Sciences, Institute of Materials and Environmental Chemistry, Hungarian Academy of Sciences, 1117, Budapest Magyar tudósok krt. 2, Hungary*
[4] *Department of Thermal and Nuclear Power Engineering, Technical University of Sofia, 8 Kl. Ohridsky Blvd., 1000 Sofia, Bulgaria*

Submitted on July 21, 2016; Revised on November 22, 2016

In this study it was demonstrated for the first time that the application of silver modified nanoporous silica as a carrier of natural flavonoid quercetin leads to the formation of efficient dermal formulation. By direct or post synthesis methods finely dispersed silver nanoparticles can be stabilized in the channels or on the outer surface of nanoporous silica support. High quercetin loading capacity (over 40 wt. %) could be achieved on the parent and Ag-containing MCM-41 samples. The in vitro release process at pH=5.5 showed slower quercetin release from Ag-modified MCM-41 samples compared to the parent one. The cytotoxic experiments evidenced that quercetin encapsulated in Ag-modified silica carriers has superior antineoplastic potential against HUT-29 cells compared to free drug.

Keywords: silver, quercetin, nanoporous silica, spherical MCM-41.

INTRODUCTION

In the recent years several efficient nanoporous silica based drug delivery systems have been developed [1,2]. Nanoporous silica carriers (SBA-15 or MCM-41) are biocompatible materials and have the capability both to load nanosized metal particles into the channels and to be functionalized with organic groups [3,4]. The functionalization of the silica surface (inside the channels and/or the outer surface) not only can enhance the adsorption of drug molecules but give opportunities to modify the release properties. The effect of modified drug release can be combined with the antibacterial effect of metallic nanoparticles, such as silver. From antiquity silver has been used as a disinfectant and for the treatment of burns, ulcerations and bacterial infections. The silver nanoparticles are widely explored and applied because their toxicity to human cells is quite lower than to bacteria and they had broad spectrum of antimicrobial activity and low propensity to induce bacterial resistance [5]. Silver nanoparticles can be stabilized in the channels or on the outer surface of mesoporous silica supports, and besides the empty channels can be loaded by biologically active molecules.

Flavonoids are natural pigments found in many plants and fruits and they possess high antioxidative and antiradical activities. Quercetin (2-(3,4-dihydroxyphenyl)-3,5,7-trihydroxy-4H-chromen-4-one, Fig. 1) is the most widespread flavonoid with the highest antioxidant activity among flavonoids. It was chosen in our study due to its interesting biological and pharmacological effects, such as anti-inflammatory, antiallergenic, antiviral, antibacterial and anticancer [6]. Biological activity of the quercetin is characterized by multiple mechanisms, including scavenging reactive oxygen species (ROS) [7], inhibition of lipid peroxidation [8], and chelating metal ions [9].

Due to their potential beneficial effects in the prevention of oxidative stress, antioxidants are studied not only for oral administration but also for dermal applications for protection against UV radiation damage [10,11] or for prevention of skin cancer [12,13]. Their use as pharmaceutical agents is extremely limited by their low water solubility and high instability in a neutral and alkaline medium [14]. To overcome this major hurdle and to increase quercetin's bioavailability, quercetin was loaded in delivery systems on the basis of mesoporous silica materials.

In this study silver nanoparticle containing mesoporous silica MCM-41 carriers, prepared by direct synthesis or post synthesis method, were loaded with quercetin. *In vitro* release profiles of quercetin from parent and Ag modified mesoporous silica particles were studied in respect of their possible application as dermal formulations against

* To whom all correspondence should be sent:
E-mail: ivtrendafilova@gmail.com

cutaneous T-cell lymphoma. The cytotoxic potential of non-loaded and quercetin loaded particles was investigated against two types of human cells, including HUT-29 cells as a model of CTCL *in vitro*.

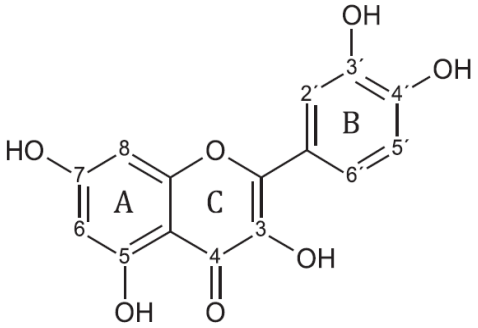

Figure 1 Molecular structure of quercetin.

EXPERIMENTAL

Materials

Cetyl trimethyl ammonium bromide (CTAB), Quercetin (>99.5%) and tetraethyl orthosilicate (TEOS) were purchased by Aldrich.

Synthesis of siliceous MCM-41 material

Spherical nanosized (100 nm) MCM-41 particles were prepared according to the procedure of Huh et al. [15]. This sol-gel procedure is carried out at 80°C in water solution with NaOH as a catalyst. The silica source was tetraethyl orthosilicate (TEOS), and hexadecyltrimethyl-ammonium bromide (C_{16}TMABr) was applied as template. The relative molar composition of the reaction mixture was: 1 TEOS: 0.12 C_{16}TMABr: 0.31 NaOH: 1190 H_2O. The formed gel was aged at 80°C for 2 h, than washed with distilled water until neutral pH, and dried at ambient. Template was removed by heat treatment in air at 450°C for 5h with a heating ramp of 1°C/min.

Direct synthesis of Ag-MCM-41

Silver nanoparticles were loaded to the silica carrier by the template ion-exchange method of Gac et. al.[**Error! Bookmark not defined.**]. The template containing MCM-41 material was ion-exchanged by refluxing it at 80°C with 0.036 M $AgNO_3$ solution (50 ml/g MCM-41) for 20 h, and then filtered on 0.2 μm membrane filter, and washed with distilled water. The ion-exchanged material was heat treated in air at 550°C for 5 h with a heating rate of 1°C/min. Silver containing MCM-41 sample prepared by template ion-exchange method was designated as Ag-MCM-41(DS).

Post synthesis modification of MCM-41 with Ag

Modification of MCM-41 with $AgNO_3$ by incipient wetness impregnation technique was applied for loading of 2, 4 and 5.5 wt. % silver. In a typical experiment silver nitrate – 9.45 mg, 18.9 mg and 25.9 mg for 2, 4 and 5.5 wt. % silver, respectively, was dissolved in 1 ml ethanol (99.9%) and 300 mg of mesoporous support (MCM-41) were added. The functionalization was performed at room temperature. Samples were calcined in air at 450°C for 3 hours and designated as xAgMCM-41(PS) where x= 2,4 or 5.5 wt.% Ag.

Loading of quercetin on silver modified nanoporous MCM-41 materials

Ag modified materials and quercetin in ratio 1:1 were stirred in 1 ml ethanol (99.9%) and then dried at 50°C till the total evaporation of the solvent. The quercetin loaded MCM-41 formulation was designated as AgMCM-41(DS)Qu, and xAgMCM-41(PS)Qu, where *x*= 2, 4 and 5.5 Ag wt.%.

Characterization of the samples

X-ray patterns were recorded by a Philips PW 1810/3710 diffractometer with Bregg-Brentano parafocusing geometry applying monochromatized CuKα (λ=0.15418 nm) radiation (40 kV, 35 mA) and a proportional counter.

Nitrogen physisorption measurements were carried out at 77 K using TriStar II surface area analyzer, Micrometrics. The specific surface area was calculated applying BET (Brunauer–Emmett–Teller) method to the monolayer adsorption region on the isotherms observed in the range of relative pressures p/p_o from 0.02 to 0.1. The pore-size distribution was calculated from desorption branch of the isotherms with the BJH (Barrett-Joyner-Halenda) method. Silica samples were pre-treated at 200°C, whereas drug loaded materials at 80°C for 5 h before measurements [17,18].

TEM images were taken by using a MORGAGNI 268D (100 kV; W filament; point-resolution = 0.5 nm) electron microscope. Samples were suspended in small amount of ethanol and a drop of suspension was deposited onto copper grid covered by carbon supporting film and dried at ambient.

Thermogravimetric measurements were performed with a Setaram TG92 instrument with a heating rate of 5 °C/min in air flow.

In-vitro release study

An in-vitro quercetin release study was performed in buffer (pH = 5.5) at 37°C. The drug-loaded particles (2 mg) were incubated in 200 ml phosphate buffer with pH=5.5 at 37°C under stirring (300 rpm). At appropriate time intervals, 3 ml samples were withdrawn from the release

medium and analyzed with UV-Vis spectroscopy at a wavelength of 367 nm. The concentration of the released quercetin was calculated according to the standard curves prepared in pH=5.5 solution ($r>0.9993$).

Cell lines and culture conditions

The cell lines HEK-293 (human embryonal kidney cells) and HUT-78 (cutaneous T-cell lymphoma - CTCL) were supplied by DSMZ GmbH, Germany. Cells were cultured routinely in a controlled environment: 37°C in 5% CO_2 humidified atmosphere. All cell lines were maintained in RPMI 1640 supplemented with 2 mM L-glutamine and 10% fetal calf serum. The cell lines were subcultured biweekly to maintain continuous logarithmic growth.

Cytotoxicity assay

Cell survival was evaluated by using the standard MTT-dye reduction assay (Mosmann, 1983) with slight modifications (Konstantinov et al., 1999). The method is based on the ability of viable cells to metabolize a yellow tetrazolium salt to a violet formazan product which is detected spectrophotometrically at 527 nm. Exponentially growing cells were plated in 96-well sterile plates at a density of 10^4 cells/ well in 100 μL of medium and were incubated for 24 h. Thereafter the quercetin and the tested mesoporous silica particles were applied for 72 h, whereby for each concentration a set of 8 wells was used. After a 72-h continuous exposure period, 10 μL aliquots from a 5 mg/ml MTT solution were added to each well and the plates were further incubated for 4 h at 37°C in a humidified 5 % CO_2 atmosphere. The formazan crystals yielded were solubilized by addition of a 5% solution of HCOOH in isopropanol. The MTT-formazan absorbance was read on a microprocessor controlled multiplate reader (Labexim LMR-1). The cell survival data were normalized as percentage of the untreated control (set as 100% viability) and were fitted to sigmoidal dose response curves and the corresponding IC_{50} values (concentrations causing 50% suppression of cellular viability) were calculated.

RESULTS AND DISCUSSION

Material characterization

Low and high angle XRD powder patterns of pure silica and silver containing MCM-41 materials, and their Qu loaded varieties are shown in Fig. 1. AgMCM-41 samples prepared by template ion-exchange method or post synthesis modification show the typical patterns of highly ordered hexagonal phase. The intensity of (100) reflection is lower than that of parent silica material indicating some decrease of structure ordering after modification with Ag. More significant intensity decrease and broadened reflections are observed for the functionalized and quercetin loaded mesoporous samples, indicating some loss of structure ordering or pore filling (not shown).

Reflection characteristic of the crystalline form of Ag could be observed only for AgMCM-41 prepared by direct synthesis and 5.5AgMCM-41 prepared by post synthesis method. For other samples containing lower amount of Ag, crystalline Ag was not registered (Fig.1 A).

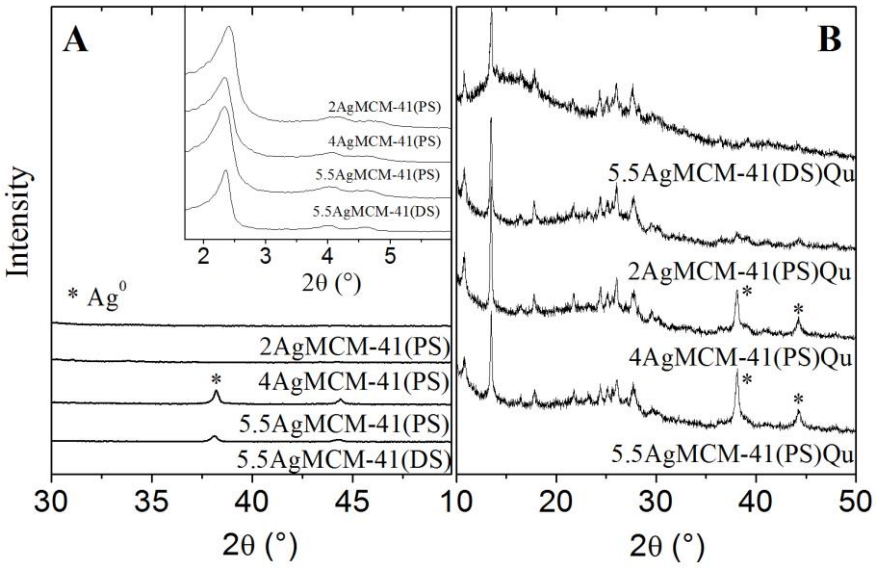

Fig. 1 XRD patterns of silver containing nanoporous pure silica and silver modified silica samples (A) and their Qu loaded varieties (B).

High angle XRD patterns of quercetin loaded parent and silver modified silica carriers are shown in Fig. 1 B. Reflections of quercetin can be observed on all samples. This is evidence that quercetin is not only contained in the pore channels, but can be found on the outer surface of the small nanoparticles or in the voids among the particles. Quercetin can be found in its anhydrous form after loading due to its recrystallization in the ethanolic media.

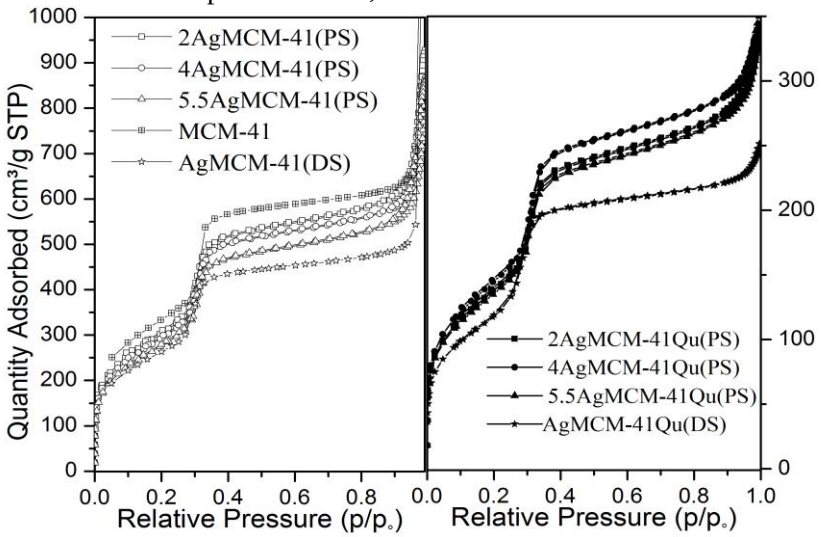

Fig. 2 N_2 physisorption isotherms of pure silica, silver containing and quercetin loaded varieties of nanoporous silica materials.

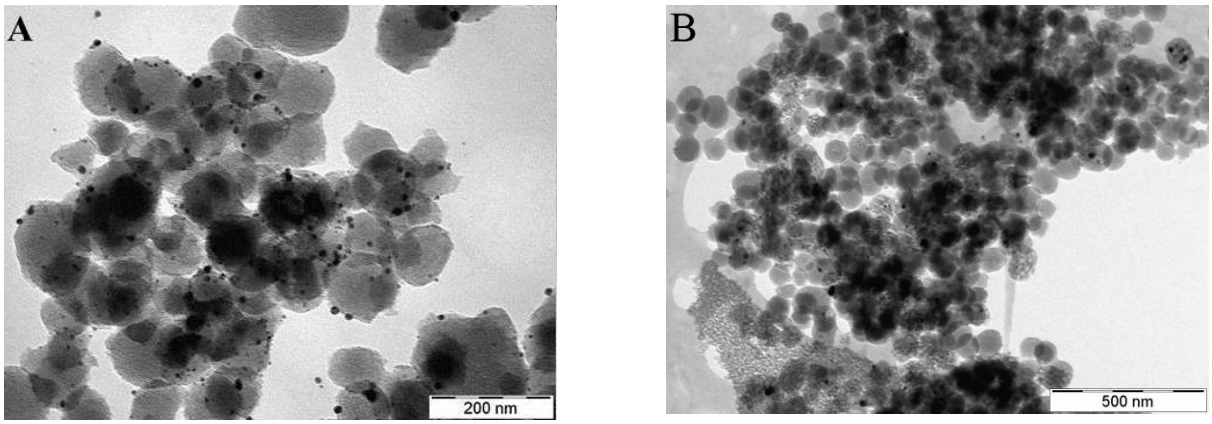

Fig. 3 TEM images of 5.5AgMCM-41(DS) (A) and 4AgMCM-41(PS) (B) samples

The above observations were supported also by the N_2 adsorption data (Fig. 2). Textural parameters are summarized in Table 1. The isotherms of pure silica and silver modified MCM-41 materials exhibited a sharp increase at a relative pressure of p/po= 0.2-0.4, which was associated with capillary condensation in the channels and narrow pore size distribution (Fig. 2). The isotherms of the MCM-41 samples were reversible and did not show any hysteresis loop. Specific surface area and the total pore volume of Ag-modified MCM-41 sample are slightly lower in comparison with the parent material. However, after quercetin loading textural parameters of the samples show a significant decrease in the surface area and total pore volume, due to the macrovoid filling revealed by the slower adsorption at high p/p_o.

The modification by silver does not influence the original morphology of MCM-41 material as evidenced by TEM investigations (Fig. 3). AgMCM-41 and 5.5AgMCM-41 (Fig.3) show the typical 100 nm spherical particles and the channel system is well preserved. Silver nanoparticles with different dispersity, among 5-20 nm, can be observed on the images. These results are in accordance with XRD results showing the presence of separate silver phase on the outer side of the particles.

Diffuse reflectance UV-Vis spectroscopic investigation evidenced the formation of Ag nanoparticles and incorporation of Ag into the silica matrix. UV-Vis spectra of the parent and the silver modified silica carriers can be seen in Fig. 4. The spectra of the samples prepared by post synthesis method show an intensive peak at around 400 nm

which is due to the formation of Ag nanoparticles [19, 20]. The registered peak at 280 nm in the spectrum of AgMCM-41 can be assigned to the presence of silver ions [19].

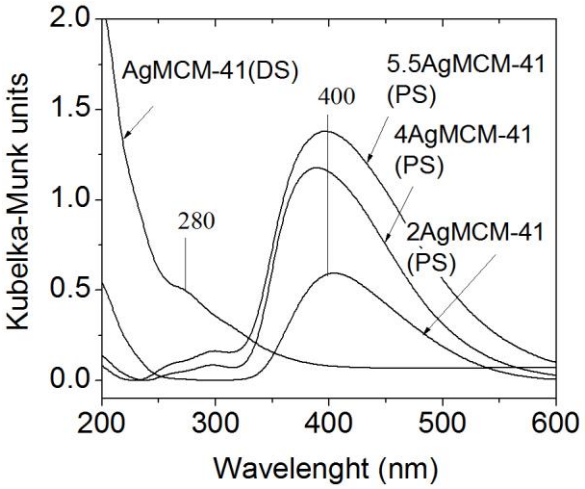

Fig.4 UV Vis spectra of the studied silver containing MCM-41 samples.

Adsorption of quercetin

Quercetin was adsorbed on silver containing samples by dissolving it in ethanol (99.9%). Qu penetrated into the channels of silica carrier and partial pore filling was achieved, evidenced by the N_2 physisorption data (Fig 2, Table 1). However, according to the XRD patterns of the Qu loaded silica materials (Fig. 1 B) some amount of Qu can be found as a separate phase in the sample as well. The amount of quercetin loaded in the mesopores of Ag-modified MCM-41 was quantified using thermogravimetry (TG, Fig 5). TG data are presented in Table 1. The studied samples showed high loading capacity of quercetin (44 -50 wt. %) The loaded amount of quercetin is higher for the silver modified sample prepared by direct synthesis (50 wt.%).

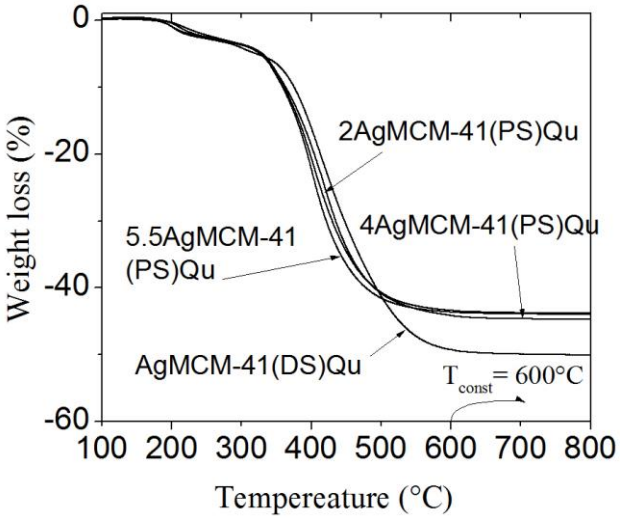

Fig. 5 Thermogravimetric curves of Qu loaded silver MCM-41 samples.

Table 1. Composition and textural properties of the studied samples.

Samples	a_0[a] (nm)	Qu content (mg/g)	BET surf. area (m^2/g)	Total pore vol. (cm^3/g)	PD[b] (nm)
MCM-41	4.4	-	1175	0.970	2.7
AgMCM-41(DS)	4.3	-	927	0.760	2.6
2AgMCM-41(PS)	4.2	-	1170	0.820	2.7
4AgMCM-41(PS)	4.3	-	1162	0.790	2.7
5.5AgMCM-41(PS)	4.3	-	1097	0.750	2.8
AgMCM-41(DS)Qu	4.3	50.0	430	0.371	2.6
2AgMCM-41(PS)Qu	4.2	44.0	539	0.380	2.8
4AgMCM-41(PS)Qu	4.2	44.7	568	0.400	2.8
5.5AgMCM-41(PS)Qu	4.1	44.0	530	0.370	2.8

[a] Unit cell parameter ($a_0 = 2d_{100}(3)^{-1/2}$).
[b] Mean pore diameter calculated by the BJH method.

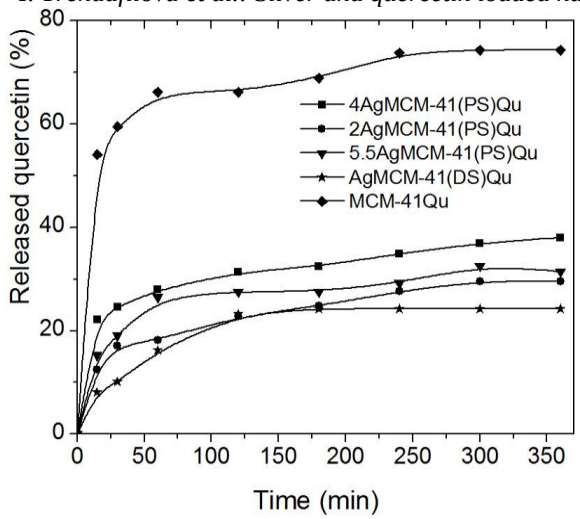

Fig. 6 *In vitro* release of quercetin from parent and Ag-modified MCM-41 carriers.

In vitro release of quercetin

The *in vitro* release of Qu from all samples was investigated in a phosphate buffer (pH=5.5). The latter pH value is widely applied for *in vitro* experiments for dermatological formulations. The drug release profiles are presented in Fig. 6. As evident from the presented data the parent mesoporous MCM-41 silica are characterized with burst quercetin release where over 60 % of the encapsulated quercetin is released within 30 minutes. Contrary, the silver-modified silica formulations' showed slower drug release and thus within 6 h the Qu release reached not more the 36 %. Probably the main part of quercetin remains in the pores of the silica carrier.

Cytotoxicity assessment

The cytotoxicity potential of mesoporous silica non-modified or Ag-modified nanoparticles was determined in two human cell lines with different cell type and origin, namely non-malignant HEK-293 and malignant HUT-78. The two cell lines were chosen in order to discriminate between the growth inhibitory potential of tested systems against non-tumorigenic and malignant cell lines, as the lack of toxicity is an important requirement for all materials used in preparation of drug delivery systems. In addition a comparative evaluation of the cytotoxic effect of quercetin loaded system vs. free drug (ethanol solution) in the above mentioned cell lines was performed. HEK-293 cells represent non-cancerous epithelial cells, whereas HUT-78 are a suitable model for cutaneous T-cell lymphoma.

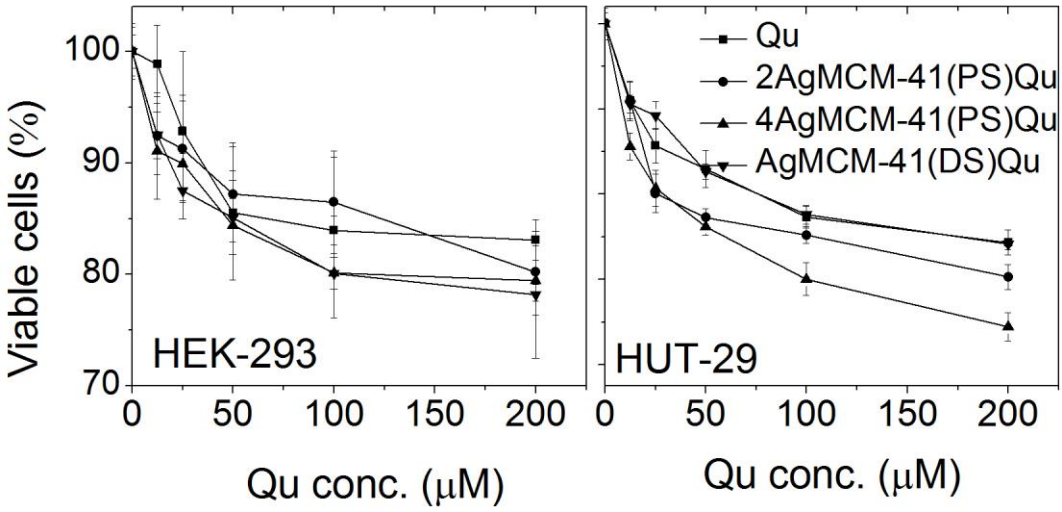

Fig. 7. The concentration-response curves determined by the MTT-dye reduction assay after 72 hours continuous exposure. Concentration range of 25-200 μM quercetin corresponds to 0.2-1 mg/ml of mesoporous silica particles. Each data point represents the arithmetic mean ± SD of 8 separate experiments.

Table 2 Equieffective concentrations of tested quercetin formulations, *vs.* the free drug.

Cell line	IC_{50} (μM)			
	Quercetin (Qu)	2AgMCM-41Qu (PS)	4AgMCM-41Qu (PS)	AgMCM-41Qu (DS)
HEK-293	n.d.	n.d.	n.d.	n.d.
HUT-78	174.8	105.53	59.6	68.4

The growth inhibitory concentration-response curves are presented in Fig. 7 and the corresponding equieffective IC 50 values are summarized in Table 2. Evident from the growth inhibitory concentration-response curves shown in Fig. 7, the non-loaded silica particles, as well as their quercetin loaded counterparts and quercetin itself, failed to induce any significant decrease in

cell viability of non-malignant HEK-293 cells even at the highest dose of 200 μM and furthermore in the whole tested concentration range IC_{50} were not reached (Table 2). In contrast in malignant HUT-78 cells all tested formulations exerted clear concentration dependent cytotoxic effect. These findings show that the tested compounds are characterized with high selectivity against malignant cells and are non-harmful for normal cells. In addition to their selectivity quercetin loaded mesoporous silica nanoparticles were superior in terms of cytotoxic activity as compared to the free drug. The concentration-response curves were shifted to the lower concentrations and respectively the IC_{50} values were app. two folds lower as compared to those of free quercetin, applied as an ethanol solution. This effect was more pronounced in quercetin loaded 4AgMCM-41 particles prepared by direct synthesis, causing more than 60 % eradication of viable cells at the highest concentration.

CONCLUSIONS

In this study it was shown that silver modified MCM-41 materials are suitable carriers for bioflavanols, such as quercetin, to design dermal delivery systems. It was found that nanoporous silica materials can be easily modified by direct or post-synthesis methods to prepare silver nanoparticles inside the channels or on the outer surface of the particles. Incipient wetness impregnation method was used for quercetin loading on parent and Ag-modified mesoporous carriers. High quercetin loading capacity (over 40 wt. %) was registered on all samples. The in-vitro release process at pH=5.5 showed lower and incomplete quercetin release for silver modified samples in comparison with the parent MCM-41 possibly due to the formation of complex between quercetin and Ag. High quercetin loading and controlled release indicate that the obtained delivery systems are promising for dermal application. The cytotoxic experiments show that quercetin encapsulated in Ag-modified silica carrier (4 wt. % Ag) prepared by post synthesis proved to exert superior antineoplastic potential against HUT-29 cells compared to free drug.

Acknowledgements: *Financial support by the Bulgarian-Hungarian Inter-Academic Exchange Agreement is greatly acknowledged. I. Trendafilova thanks the ДФНП-191/14.05.2016 project for young scientists support funded by the Bulgarian Academy of Sciences. S. Boycheva acknowledged the Alexander von Humboldt Foundation for surface analyzer equipment donation.*

REFERENCES

1. M. Vallet-Regi, A. Ramila, R.P. del Real, J. Perez-Pariente, *Chem. Mater.* **13**, 308 (2001).
2. Sh. Wang, *Micropor. Mesopor. Mater.* **117**, 1 (2009).
3. A.Szegedi, M. Popova, I. Goshev, Sz. Klébert, J. Mihály, *J. Solid State Chem.* **194**, 257 (2012).
4. M. D. Popova, Á. Szegedi, I. N. Kolev, J. Mihály, B. S. Tzankov, G. Tz. Momekov, N. G. Lambov, K. P. Yoncheva, *Int. J. Pharm.* **436**, 778 (2012).
5. M. Rai, A. Yadav, A. Gade, *Biotechnol. Adv*. **27**, 76 (2009).
6. M. Zhang, S.G. Swarts, L. Yin, C. Liu, Y. Tian, Y. Cao, M. Swarts, S. Yang, S.B. Zhang, K. Zhang, Oxygen Transport to Tissue XXXII, Springer, 283 (2011).
7. V. Krishnamachari, L.H. Levine, P.W. Paré, *J. Agric. Food Chem.*, **50**, 4357 (2002).
8. O. Dangles, C. Dufour, G. Fargeix, *J. Chem. Soc*., **2**, 1215 (2000).
9. Z. Jurasekova, A. Torreggiani, M. Tamba, S. Sanchez-Cortes, J. Garcia-Ramos, *J. Mol. Struct.*, **918**, 129 (2009).
10. R. Casagrande, S.R. Georgetti, W.A. Verri Jr., D.J. Dorta, A.C. dos Santos, M.J.V. Fonseca, *J. Photochem. Photobiol.*, **B 84**, 21 (2006).
11. D. Liu, H. Hu, Z. Lin, D. Chen, Y. Zhu, S. Hou, X. Shi, *J. Photochem. Photobiol.*, **B 127**, 8 (2013).
12. M.M. Heinen, M.C. Hughes, T.I. Ibiebele, G.C. Marks, A.C. Green, J.C. van der Pols, *Eur. J. Cancer* **43**, 2707 (2007).
13. J.S. Reis, M.A. Corrêa, M.C. Chung, J.L. dos Santos, *Bioorg. Med. Chem*. **22**, 2733 (2014).
14. A.J. Smith, P. Kavuru, L. Wojtas, M.J. Zaworotko, R.D. Shytle, *Mol. Pharm.* **8,** 1867 (2011).
15. S. Huh, J. Wiench, J.-Ch Yoo, M. Pruski, V.S.-Y. Lin, *Chem. Mater.* **15**, 4247 (2003).
16. W. Gac, A. Derylo-Marczewska, S. Pasieczna-Patkowska, N. Popivnyak and G. Zukocinski, *J. Mol. Catal. A: Chem.*, **268**, 15 (2007).
17. A. Szegedi, M. Popova, I. Goshev, J. Mihaly, *J. Solid State Chem.* **184**, 1201 (2011).
18. A.Szegedi, M. Popova, K. Yoncheva, J. Makk, J. Mihaly, P. Shestakova, *J. Mater. Chem. B* **2**, 6283 (2014).
19. L. Jia, S. Zhang, F. Gu, Y. Ping, X. Guo, Z. Zhong, F. Su, *Microporous Mesoporous Mat.* **149**, 158 (2012).
20. W. Zhu, Y. Han, L. An, *Microporous Mesoporous Mat.* **80,** 221 (2005).

МОДИФИЦИРАНИ СЪС СРЕБРО НАНОСТРУКТУРНИ СИЛИКАТНИ МАТЕРИАЛИ, НАТОВАРЕНИ С КВЕРЦЕТИН, КАТО ПОТЕНЦИАЛНИ ДЕРМАЛНИ ПРЕПАРАТИ

Ив. Трендафилова[1]*, Д. Момекова[2], А. Сегеди[3], Г. Момеков[2], Д. Згурева[4], С. Бойчева[4], М. Попова[1]

[1]*Институт по органична химия с Център по фитохимия, БАН*
[2] *Фармацевтичен факултет, Медицинска академия, София*
[3]*Изследователски център по природни науки, Институт по материали и химия на околната среда, Унгария*
[4] *Катедра топлотехника и ядрена енергетика, Технически университет, София*

Постъпила на 21 юли, 2016 г. коригирана на 22 ноември, 2016 г.

(Резюме)

В настоящото изследване за първи път модифициран със сребро MCM-41 силикат е използван, като носител на природния флавоноид кверцетин и на негова основа е разработена ефикасна лекарствена форма. Чрез директен синтез или постсинтезен метод са получени и стабилизирани финно дисперсни сребърни наночастици в порите или върху външната повърхност на нанопорестия силикат. Постигната е висока степен на натоварване с кверцетин (над 40%) както при изходните, така и при сребро-съдържащи образци. In-vitro тестовете при pH=5.5 показват забавено освобождаване на кверцетина от модифицираните със сребро MCM-41 проби, в сравнение с немодифицирните. Цитотоксичните експерименти показват, че кверцетинът натоварен в модифицирани със сребро силикатни носители има по-висок антинеопластичен потенциал срещу HUT-29 клетки в сравнение с чистото вещество.